Title

Subthalamic local field potentials in Parkinson's disease and isolated dystonia: An evaluation of potential biomarkers

Authors

Wang, Doris D
de Hemptinne, Coralie
Miocinovic, Svjetlana
et al.

Publication Date

2016-05-01

DOI

10.1016/j.nbd.2016.02.015

Peer reviewed

Neurobiology of Disease 89 (2016) 213–222

Contents lists available at ScienceDirect

Neurobiology of Disease

journal homepage: www.elsevier.com/locate/ynbdi

Subthalamic local field potentials in Parkinson's disease and isolated dystonia: An evaluation of potential biomarkers☆,☆☆

Doris D. Wang [a,*], Coralie de Hemptinne [a], Svjetlana Miocinovic [b], Salman E. Qasim [a], Andrew M. Miller [a], Jill L. Ostrem [b], Nicholas B. Galifianakis [b], Marta San Luciano [b], Philip A. Starr [a]

[a] Department of Neurological Surgery, University of California San Francisco, San Francisco, CA, USA
[b] Department of Neurology, University of California San Francisco, San Francisco, CA, USA

ARTICLE INFO

Article history:
Received 19 November 2015
Revised 7 February 2016
Accepted 10 February 2016
Available online 14 February 2016

Keywords:
Deep brain stimulation
Phase amplitude coupling
Beta oscillation
Electrophysiology
Cross frequency interaction

ABSTRACT

Local field potentials (LFP) recorded from the subthalamic nucleus in patients with Parkinson's disease (PD) demonstrate prominent oscillations in the beta (13–30 Hz) frequency range, and reduction of beta band spectral power by levodopa and deep brain stimulation (DBS) is correlated with motor symptom improvement. Several features of beta activity have been theorized to be specific biomarkers of the parkinsonian state, though these have rarely been studied in non-parkinsonian conditions. To compare resting state LFP features in PD and isolated dystonia and evaluate disease-specific biomarkers, we recorded subthalamic LFPs from 28 akinetic-rigid PD and 12 isolated dystonia patients during awake DBS implantation. Spectral power and phase-amplitude coupling characteristics were analyzed. In 26/28 PD and 11/12 isolated dystonia patients, the LFP power spectrum had a peak in the beta frequency range, with similar amplitudes between groups. Resting state power did not differ between groups in the theta (5–8 Hz), alpha (8–12 Hz), beta (13–30 Hz), broadband gamma (50–200 Hz), or high frequency oscillation (HFO, 250–350 Hz) bands. Analysis of phase-amplitude coupling between low frequency phase and HFO amplitude revealed significant interactions in 19/28 PD and 6/12 dystonia recordings without significant differences in maximal coupling or preferred phase. Two features of subthalamic LFPs that have been proposed as specific parkinsonian biomarkers, beta power and coupling of beta phase to HFO amplitude, were also present in isolated dystonia, including focal dystonias. This casts doubt on the utility of these metrics as disease-specific diagnostic biomarkers.

Published by Elsevier Inc.

1. Introduction

Excessive oscillatory activity in the basal ganglia-thalamocortical circuit may be a major component of the pathophysiology of parkinsonian motor signs. Manifestations of excessive oscillatory activity may include theta (5–8 Hz), alpha (8–12 Hz), or beta (13–30 Hz) band oscillations in single unit discharge (Bergman et al., 1994; Moran et al., 2008), oscillatory synchronization between simultaneously recorded neurons (Hanson et al., 2012; Levy et al., 2002; Nini et al., 1995), and exaggerated spike field synchrony (Moran et al., 2008; Shimamoto et al., 2013; Weinberger et al., 2006). One way to study oscillatory activity in Parkinson's disease (PD) is to record the local field potential (LFP) from implanted basal ganglia electrodes intraoperatively or during a brief postoperative period when leads may be temporarily externalized (Galvan et al., 2015; Hammond et al., 2007). Local field potentials are thought to represent summed, synchronized subthreshold activity from pools of neurons near the recording electrodes. Subthalamic nucleus (STN) LFPs in PD patients show prominent beta oscillatory activity, whose amplitude is suppressed by levodopa and by STN deep brain stimulation (DBS) in a manner that correlates with symptom improvement (Bronte-Stewart et al., 2009; Chen et al., 2007; Kuhn et al., 2008; Little et al., 2012; Wingeier et al., 2006). This has led to the hypothesis that STN beta band oscillations may contain biomarkers diagnostic of the parkinsonian state, and that these features could be used for potential control signals for closed-loop DBS (Little et al., 2013; Stanslaski et al., 2012).

Specific features of the STN LFP that have been proposed as potential diagnostic parkinsonian biomarkers include beta band power (Little et al., 2013) and coupling of beta phase to the amplitude of high frequency oscillations (HFOs, 250–350 Hz), one form of phase-amplitude coupling (Lopez-Azcarate et al., 2010). If true, then these metrics should

☆ Authors' contributions and conflict of interest disclosures: Authors report no conflict of interest.

☆☆ Acknowledgment: This work was supported by NIH R25 PAR-13-384 NINDS grant and R01 NS090913-01.

* Corresponding author at: 505 Parnassus, M779, Department of Neurological Surgery, University of California San Francisco, Box 0112, San Francisco, CA 94143-0112, USA.
E-mail addresses: Doris.Wang@ucsf.edu (D.D. Wang), Coralie.Dehemptinne@ucsf.edu (C. de Hemptinne), Svjetlana.Miocinovic@ucsf.edu (S. Miocinovic), Salman.Qasim@columbia.edu (S.E. Qasim), Andrew.Miller@ucsf.edu (A.M. Miller), Jill.Ostrem@ucsf.edu (J.L. Ostrem), Nicholas.Galifianakis@ucsf.edu (N.B. Galifianakis), Marta.SanLucianoPalenzuela@ucsf.edu (M.S. Luciano), Philip.Starr@ucsf.edu (P.A. Starr).

Available online on ScienceDirect (www.sciencedirect.com).

http://dx.doi.org/10.1016/j.nbd.2016.02.015
0969-9961/Published by Elsevier Inc.

differ between patients with PD and those with non-parkinsonian conditions. However, STN LFP characteristics in non-parkinsonian conditions have rarely been studied (Bastin et al., 2014; Danish et al., 2007) and never compared directly to those of PD patients. Here, we report the first large series (N = 12 patients) of STN LFP recordings in isolated dystonia, and compare them to similar recordings in 28 patients with akinetic-rigid PD. We found that both PD and dystonia patients had STN LFPs whose power spectra had a peak in the beta range, without significant differences in amplitude or the frequency of peak power. Coupling between STN LFP beta phase and the amplitude of HFOs was found in both PD and isolated dystonia patients. Our findings suggest that neither beta power nor phase-amplitude coupling within the STN is a diagnostic biomarker for the parkinsonian state. Our study does not refute the potential utility of these oscillatory features of the STN LFP as markers of response to therapy in PD.

2. Methods

2.1. Patients

Patients with Parkinson's disease and isolated dystonia were recruited from the movement disorders surgery clinics at the University of California San Francisco or the San Francisco Veteran Affairs Medical Center. All patients were scheduled to undergo implantation of deep brain stimulator electrodes into the STN, and underwent evaluation for motor impairments within 30 days prior to surgery using the Unified Parkinson's Disease Rating Scale motor subscale (UPDRS-III) in the off- and on- medication states (for PD patients), or the Toronto Western Spasmodic Torticollis Rating Scale and Burke–Fahn–Marsden Dystonia Rating Scale (for dystonia patients). Inclusion criteria were the following: for PD patients, akinesia and rigidity as the most prominent symptoms with UPDRS-III > 20 in the off state and absent or minimal observed tremor during intraoperative recording; for isolated dystonia patients, those with focal cervical dystonia, segmental craniocervical dystonia or generalized dystonia without evidence for acquired etiology. Dystonia patients in this physiology study were also participating in a prospective clinical trial of the efficacy of STN DBS for isolated dystonia (Ostrem et al., 2011). Informed consent was obtained prior to surgery under a protocol approved by the Institutional Review Board. Data from a subset of these patients has been published previously (de Hemptinne et al., 2013).

2.2. DBS electrode implantation in PD and dystonia patients

Surgical planning and placement of DBS electrodes in the subthalamic nucleus (STN) were performed using methods previously described (Ostrem et al., 2011; Starr, 2002). Briefly, the intended STN target location was identified as a T2 hypointense area immediately lateral to the anterior margin of the red nucleus and superior to the lateral region of the substantia nigra pars reticulata (approximately 12 mm lateral, 3 mm posterior, and 4 mm inferior to the mid commissural point, which is the midpoint of the line connecting the anterior and posterior commissures) (Fig. 1A). All surgeries were performed in the awake resting state after discontinuation of propofol for at least 30 min. Microelectrode recordings (MER) were performed to map movement-related single cells, and borders of the STN were defined based on the MER map. A DBS lead (Medtronic model 3389 for all patients except PD patient #2, who had a 3387 lead) was then placed. All DBS electrodes were placed with contact 0 in ventral STN, contact 3 above the dorsal border and contacts 1 and 2 in the motor territory. LFPs were recorded from the motor territory in the bipolar configuration with contact 1 as the active electrode and contact 2 as reference. Targeting was confirmed by electrical stimulation-induced symptom improvement and side effect thresholds obtained by DBS stimulation. Intraoperative computed tomography (iCT) scans computationally fused to the preoperative MRI were used to confirm correct lead location, as well as a postoperative MRI.

2.3. STN LFP recordings

All LFP recordings were performed intraoperatively after DBS electrode implantation. All anti-Parkinsonian and anti-dystonic medications were stopped at least 12 h before the start of surgery. Patients were instructed to keep their eyes open and refrain from any voluntary movements. An accelerometer was attached to the contralateral wrist to detect tremors during recording, and those with significant tremor on either review of the intraoperative video or accelerometry data were excluded from the study. The LFPs were recorded using either the Guideline 4000 system (FHC Inc., Bowdoin, ME) (n = 26, 21 PD and 5 dystonia patients) or the Alpha Omega Microguide Pro (Alpha Omega, Inc., Nazareth, Israel) (n = 14, 7 PD and 7 dystonia patients) and sampled at 1000 and 1500–3000 Hz, respectively. Bipolar STN LFPs were recorded from the physiologically identified motor territory between contacts 1 (active) and 2 (reference) of the DBS electrode. Signals were bandpass-filtered at 1–500 Hz and amplified ×7000.

2.4. Signal processing and data analysis

LFP data were processed and analyzed offline in MATLAB (Mathworks, Inc). Data were down sampled to 1 KHz and notch filtered for power line noise (60 Hz) and its harmonics (at 120, 180, 240 Hz) using a Butterworth filter. For each recording, the first 30 s free of obvious electrical noise were used for analysis. Root mean square (RMS) values were calculated.

2.5. Spectral power

Power spectral density (PSD) was calculated using the Welch periodogram method (Matlab function pwelch). For PSD calculations, we used a fast Fourier transform of 257 points (for a frequency resolution of 1.95 Hz) and 50% overlap using a Hanning window to reduce edge effects. Power of the resulting spectrogram was averaged across the following frequency bands: theta (5–8 Hz), alpha (8–12 Hz), low beta (13–20 Hz), high beta (20–30 Hz), beta (13–30 Hz), broadband gamma (50–200 Hz), and high frequency oscillations (HFO, 250-350 Hz).

2.6. Coefficient of variation

To calculate the coefficient of variation (CV) for specific spectral bands, LFP signals were bandpass filtered in the following frequency ranges: theta (5–8 Hz), alpha (8–12 Hz), low beta (13–20 Hz), high beta (20–30 Hz), beta (13–30 Hz), broadband gamma (50–200 Hz), and high frequency oscillations (HFO, 250-350 Hz). A Hilbert transform of the filtered signaled was applied and an amplitude envelope was extracted. The CV of the amplitude envelope was calculated using the following formula: CV = standard deviation (amplitude envelope)/mean (amplitude envelope).

2.7. Alpha-beta peak

Absolute measures of spectral power may differ greatly between subjects for trivial reasons, such as proximity of the recording electrode to the signal source. As a method of normalizing the properties of the alpha-beta spectral peak across subjects, spectral power in the 8–30 Hz range was normalized by “baseline” power at frequencies outside of this range. To create the “baseline” polynomial, a 5th order polynomial function was used to fit the log PSD data using the local minimum at the low frequency side of the alpha-beta peak, and values above 40 Hz and under 250 Hz (excluding noise areas around the 60 Hz harmonics). Thus, points around the alpha-beta peak areas were omitted from the

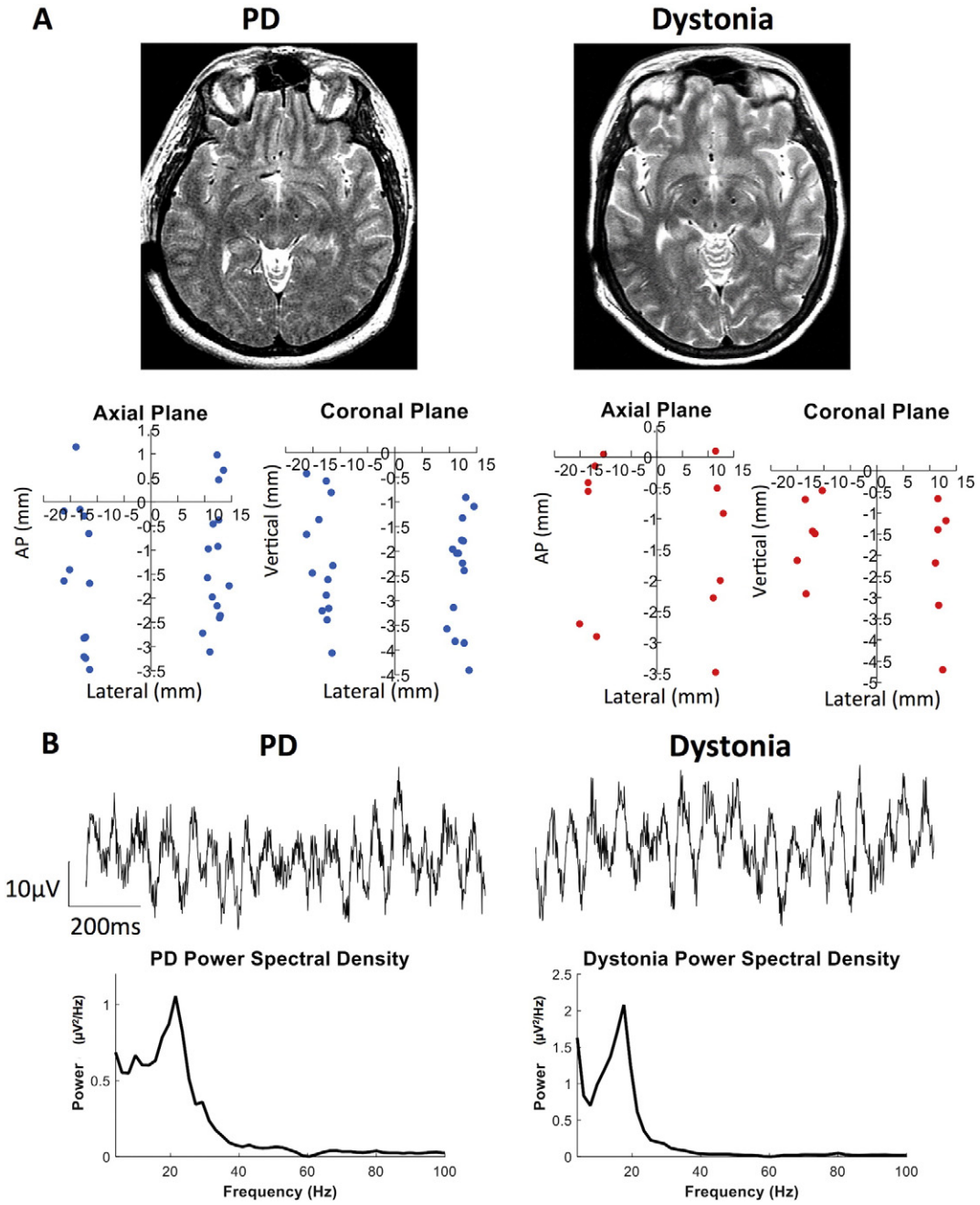

Fig. 1. — lead locations and STN LFP example recordings A) Top: Axial T2-weighted MRI showing DBS lead locations for a patient with PD (left) and dystonia (right). Bottom: axial and coronal planes showing the location of the recording contact, in mm from the midpoint between the anterior and posterior commissures in PD (left) and Dystonia (right). B) Top: one second sample resting state raw LFP signals recorded from the STN in PD (left, patient 8) and dystonia (right, patient 7). Bottom: Corresponding power spectra of a 30 s resting state LFP recording from PD and dystonia patients (from top).

polynomial fit. The difference between the log PSD and the baseline was then fitted with a Gaussian function and the resulting peak frequency, amplitude, and widths were calculated (Fig. 2C).

2.8. Phase-amplitude coupling (PAC)

We explored phase-amplitude relationship within the STN LFP using methods previously described (de Hemptinne et al., 2013; de Hemptinne et al., 2015; Tort et al., 2010). Briefly, the STN LFP signal was bandpass filtered for low frequency (4–40 Hz, with a bin bandwidth of 2 Hz) and high frequency (200–400, with a bin bandwidth of 4 Hz) using a finite impulse response filter (eegfilt_fir1 function from EEGLAB toolbox). A Hilbert transform of the filtered signal was applied, and the instantaneous phase of the low frequency components and the amplitude of the high frequency components were extracted. The distribution of the instantaneous amplitude envelope was computed for every 20° interval of the instantaneous phase. The modulation index (MI) was then calculated between the phase of low-frequency rhythm and the high-frequency amplitude by computing the entropy values of this distribution and normalizing by the maximum entropy value. A mean modulation index was calculated for each data segment by averaging MI over the phase frequency bands of interest (theta, alpha, low beta, high beta), and the amplitude frequency range of 200–400 Hz (HFO). In addition, for each frequency pair, the preferred phase was calculated by determining the interval of the instantaneous phase at which the instantaneous amplitude was maximal. Significant MI was obtained

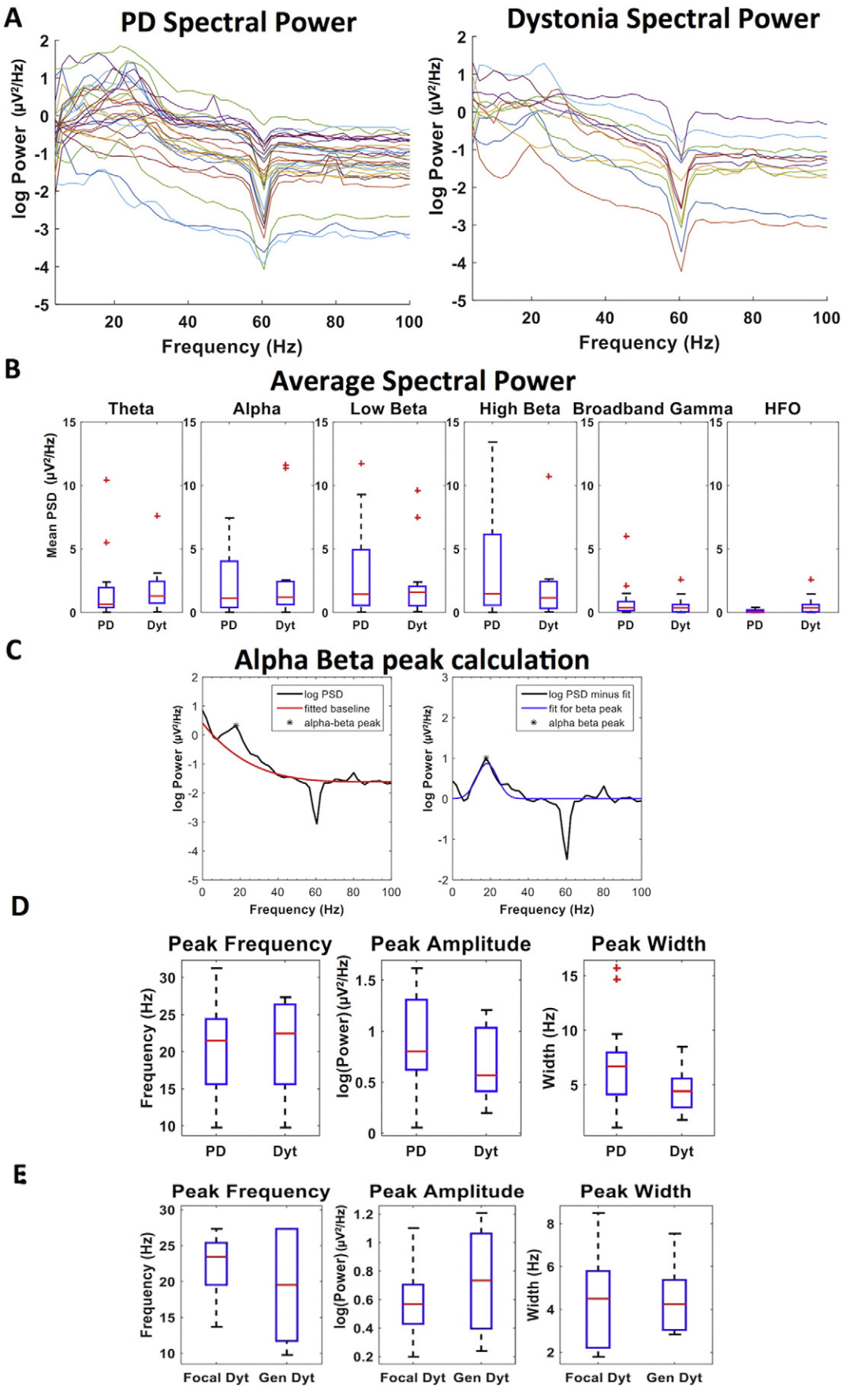
A
PD Spectral Power
Dystonia Spectral Power
log Power (μV²/Hz)
Frequency (Hz)
B
Average Spectral Power
Theta
Alpha
Low Beta
High Beta
Broadband Gamma
HFO
Mean PSD (μV²/Hz)
PD
Dyt
C
Alpha Beta peak calculation
log PSD
fitted baseline
alpha-beta peak
log PSD minus fit
fit for beta peak
alpha beta peak
log Power (μV²/Hz)
Frequency (Hz)
D
Peak Frequency
Peak Amplitude
Peak Width
Frequency (Hz)
log(Power) (μV²/Hz)
Width (Hz)
PD
Dyt
E
Peak Frequency
Peak Amplitude
Peak Width
Frequency (Hz)
log(Power) (μV²/Hz)
Width (Hz)
Focal Dyt
Gen Dyt

after finding a distribution of PAC values obtained from 100 surrogate values created by combining the instantaneous phase and amplitude with varying time lags. The 99th percentile of the distribution of these surrogate values was used as the threshold to determine significance.

2.9. Statistical analysis

The Lilliefors test (Matlab function lillietest) rejected the null hypothesis that the samples being tested came from a normal distribution, therefore the nonparametric Wilcoxon rank sum test was used to evaluate differences between PD and dystonia patients. Kuiper's test was used to assess phase angle differences (Matlab function circ_kupertest).

3. Results

3.1. Patient characteristics

We analyzed STN LFPs recorded in the resting state in 28 PD patients and 12 isolated dystonia patients. The average number of MER passes prior to DBS lead insertion was 1.3 ± 0.5 for PD and 1.3 ± 0.6 for dystonia with the majority of patients undergoing a single pass per side (20/28 PD patients and 9/12 dystonia patients). Twenty-four of twenty-eight PD patients and nine of twelve dystonia patients underwent LFP recording during the second side of a bilateral DBS implantation. Average LFP RMS voltage was 16.5 ± 9.5 μV for PD and 14.6 ± 8.6 μV for dystonia. All subjects had LFP RMS voltage >5 microvolts. Mean age was 59.5 ± 10.3 years for PD and 53.2 ± 15.0 years for dystonia. For PD patients, mean UPDRS-III off medication score was 43.9 ± 18.5 and on medication was 19.3 ± 11.1. For dystonia patients, the mean TWSTRS score was 16.3 ± 7.4 and BFMDRS score was 14.2 ± 5.3. Six of the dystonia patients had focal cervical, or segmental craniocervical forms, without any limb or trunk involvement. Clinical characteristics, including lead contact locations, for PD and dystonia patients are summarized in Tables 1 and 2, respectively. Sample postoperative MRIs showing DBS lead locations in the STN, and the coordinates of the recorded DBS contact locations in the axial and coronal planes are shown in Fig. 1A.

3.2. Similar resting state spectral power in PD and dystonia

Representative STN LFP recordings for a PD and dystonia patient and their respective power spectral densities are shown in Fig. 1B. Log transformed power spectral densities for each LFP recording in PD and dystonia patients are plotted in Fig. 2A. Spectral power analysis of a subset of patients who had longer (60-s) recordings showed minimal differences between 60-s and 30-s recordings (Supplementary Fig. 1A and B). Therefore 30-s LFP recordings were used for all subsequent analyses. Non-normalized spectral power was averaged for physiologically relevant frequency bands theta (5–8 Hz), alpha (8–12 Hz), low beta (13–20 Hz), high beta (20–30 Hz), broadband gamma (50–200 Hz), and high frequency oscillation (HFO, 250–350 Hz). There was no difference in power between PD and dystonia patients in any frequency range (Fig. 2B) (PD vs. dystonia: theta: $p = 0.2948$, alpha: $p = 0.8710$, low beta: $p = 0.8019$; high beta: $p = 0.5257$, broadband gamma: $p = 0.2948$, HFO: $p = 0.4879$; Wilcoxon rank sum test). As one method of accounting for high inter-subject variability in absolute power, we also normalized each power spectrum to the mean power between 4 and 350 Hz (Supplementary Fig. 2A). We found no differences in normalized power in any of the frequency bands (PD vs. dystonia: theta: $p = 0.0651$, alpha: $p = 0.3839$, low beta: $p = 0.4341$; high beta: $p = 0.5257$, broadband gamma: $p = 0.2948$, HFO: $p = 0.8019$; Wilcoxon rank sum test; Supplementary Fig. 2B).

Most of our LFP data were collected in a state of alert rest, which might not engage beta oscillatory phenomena in the same manner as when subjects are engaged in a motor task. To address this possibility, we studied a subset of patients (four PD and one isolated dystonia) who also participated in a study of movement related activity as previously described (de Hemptinne et al., 2015; Rowland et al., 2015). We compared each patient's LFP recordings performed during the alert rest state (awake without voluntary movement) to that recorded during the "hold" phase of a binary choice arm movement task. Analysis of spectral power during "rest" and "hold" phases revealed very small differences in beta power (mean difference of 0.0004 μV^2/Hz for PD and 0.05 μV^2/Hz for dystonia; Supplementary Fig. 3A and B).

Some recent work suggests that short bursts of beta activity may be more relevant to transitions in motor state than average beta power over longer intervals (Cagnan et al., 2015), and that the variability in these bursts are decreased in PD (Little et al., 2012). As a measure of variability in beta power we calculated the coefficient of variation (CV) of the amplitude envelope of LFP beta power, which revealed no significant difference between STN LFPs in PD and dystonia (PD vs. dystonia: 0.563 vs. 0.548, $p = 0.6902$; Wilcoxon rank sum test). Analysis of CV for other frequency bands also revealed no significant difference (PD vs. dystonia: theta, $p = 0.6591$; alpha, $p = 0.4560$; broadband gamma, $p = 0.3534$; HFO, $p = 0.0856$; Wilcoxon rank sum test).

3.3. Alpha-beta power peaks are present in PD and dystonia

Comparisons of spectral power across subjects, without normalization for signal strength (Fig. 2A and B), may be confounded by high inter-subject variability. As an additional method for characterizing the alpha-beta peak in reference to "baseline" power, we modeled the alpha-beta peak as a Gaussian in order to calculate its amplitude, width, and frequency of peak power (Fig. 2C). Using this method, we found power peaks in the alpha-beta range for all LFPs recorded, and mostly in the beta range (26 of 28 recordings in PD and 11 of 12 recordings in dystonia), with the remaining power peaks at 11.7 Hz. The median frequency of the alpha-beta peak was 21 ± 6 Hz for PD and 21 ± 7 Hz dystonia ($p = 0.7552$, Wilcoxon rank sum test; Fig. 2D, left). We also did not observe a difference between PD and dystonia in peak power amplitude ($p = 0.0954$; Wilcoxon rank sum test; Fig. 2D, middle) or width ($p = 0.1077$, Wilcoxon rank sum test; Fig. 2D, right).

3.4. STN LFP phase-amplitude coupling (PAC) is present in both PD and dystonia

Several groups have suggested that coupling between the phase of the beta rhythm and the amplitude of HFOs in the STN LFP may be related to the severity of the parkinsonian state (Lopez-Azcarate et al., 2010; Ozkurt et al., 2011). We thus tested whether STN PAC can distinguish between PD and isolated dystonia. Nineteen of the 28 PD LFPs and six of the 12 dystonia LFP recordings demonstrated PAC between alpha-beta phase and HFO amplitude, as illustrated in Fig. 3A. Comodulograms of a subset of patients who had 60-s recordings showed similar patterns of coupling in 60-s and 30-s recordings (Supplementary Fig. 4A and B). All subsequent PAC analyses were performed using 30-s LFP recordings. The Modulation index (MI), a measure of coupling, was averaged across

Fig. 2. — STN LFP spectral power characteristics in PD vs. dystonia. A) Log-transformed individual spectral power density graphs for 28 PD (left) and 12 dystonia LFP recordings (right). All signals were notch-filtered at 60 Hz. B) Boxplots (median and 25-75th quartiles) of non-normalized spectral power, averaged in specified frequency ranges for PD and dystonia showing no differences in spectral power between groups (PD vs. dystonia: theta: $p = 0.2948$, alpha: $p = 0.8710$, low beta: $p = 0.8019$; high beta: $p = 0.5257$, broadband gamma: $p = 0.2948$, HFO: $p = 0.4879$; Wilcoxon rank sum test). C) Example of method used for characterizing the alpha-beta peak (PD patient 8), to account for baseline power variations across subjects. The log spectral power (excluding the alpha-beta range) is fitted using a polynomial function to find the power baseline (red line). The resulting alpha beta peak is then fitted using Gaussian function (blue line). The power peak is indicated by *. D) Boxplots showing characteristics of the alpha-beta peak frequency, amplitude, and width. There was no significant difference between PD and dystonia (PD vs. dystonia: frequency: $p = 0.7552$; amplitude: $p = 0.0954$; width: $p = 0.1077$; Wilcoxon rank sum test). E) Boxplots showing similar alpha-beta peak characteristics between focal/segmental and generalized dystonia (Focal vs. generalized: frequency: $p = 0.5563$; amplitude: $p = 0.8182$; width: $p = 0.9172$; Wilcoxon rank sum test).

Table 1
Clinical characteristics of PD patients.

Pt #	Age	Sex	Side recorded	Disease duration (years)	PD medication	Off UPDRS-III	On UPDRS-III	Lead location[a] (mm)		
								Lat	AP	Vert
1	69	M	Left	11	Sinemet, ropinirole	68	22	−12.2	−3.2	−2.6
2	54	M	Left	6	Sinemet	42	23	−11.4	−3.5	−2.3
3	52	M	Right	11	Sinemet, trihexyphenidyl	29	27	12.7	−2.4	−3.9
4	52	M	Left	8	Sinemet, entacapone, pramipexole	>18[b]	10	−16.1	−0.2	−1.7
5	67	F	Left	19	Sinemet, selegiline, amantadine	32	21	−15.2	−1.4	−2.4
6	63	F	Right	11	Sinemet, ropinirole, amantadine	40	12	12.6	−0.4	−2.4
7	57	M	Right	7	Stalevo, sinemet, parcopa	36	11	10.6	−1.6	−2.0
8	57	F	Left	9	Sinemet, entacapone, pramipexole	52	31	−12.5	−2.8	−2.9
9	58	M	Right	9	Sinemet, entacapone, ropinirole	53	26	9.6	−2.7	−3.6
10	62	F	Right	16	Stalevo, sinemet, amantadine	92	32	12.3	1.0	−1.3
11	50	M	Right	8	Stalevo, ropinirole, rasagiline	39	7	14.5	−1.7	−1.1
12	55	F	Right	14	Sinemet, tolcapone, amantadine	22	7	11.6	−0.5	−2.0
13	54	M	Right	10	Sinemet, ropinirole, stalevo, amantadine	24	6	11.4	−2.0	−2.0
14	43	M	Right	6	Stalevo, sinemet, ropinirole	39	7	13.6	0.7	−4.4
15	68	M	Left	9	Sinemet, pramipexole, rasagiline, amantadine	40	25	−16.2	−1.6	−0.4
16	63	M	Right	15	Sinemet, entacapone, ropinirole	48	32	11.0	−3.1	−3.8
17	76	M	Left	12	Sinemet, stalevo	50	18	−13.9	1.1	−1.4
18	54	M	Left	6	Sinemet, entacapone, ropinirole	31	11	−12.1	−2.8	−3.2
19	61	M	Right	19	Sinemet, pramipexole, amantadine	31	24	12.5	−0.9	−2.2
20	73	M	Left	9	Sinemet, ropinirole, rasagiline	30	13	−12.5	−0.3	−0.6
21	67	M	Left	7	Sinemet, entacapone, pramipexole	28	7	−12.4	−3.2	−3.4
22	63	M	Left	8	Sinemet, amantadine	81	37	−13.2	−0.2	−3.2
23	30	M	Right	7	Sinemet, pramipexole, amantadine	86	51	−11.6	−0.7	−0.8
24	67	M	Right	15	Sinemet, stalevo, pramipexole, selegiline	28	11	10.7	−1.0	−3.1
25	46	M	Left	7	Sinemet, ropinirole, rasagiline, trihexyphenidyl	30	9	−11.4	−1.7	−4.1
26	59	M	Right	10	Sinemet, entacapone, pramipexole	47	16	12.3	−2.2	−1.8
27	74	M	Right	10	Sinemet	48	27	13.0	−2.4	−0.9
28	73	M	Right	20	Sinemet, tolcapone, selegiline, rotigotine, amantadine	39	18	12.6	0.5	−1.8

PD medication: Parkinson's disease medication. Lat: lateral distance from mid-commissural point; AP: anterior–posterior distance from mid-commissural point; Vert: vertical distance from mid-commissural point.
[a] Location of the recording contact in anterior commissure and post commissure plane.
[b] Patient 4 was not entirely off dopamine medication during clinical assessment and off-medication UPDRS-III score is at least 18.

alpha, low beta, and high beta phase frequency ranges for those recordings with significant PAC. The MI was highest for beta phase frequencies in both groups, and there was no difference between the disease states (alpha: $p = 0.4011$; low beta: $p = 0.2035$; high beta $p = 0.3547$; Wilcoxon rank sum test; Fig. 3B). We computed the phase frequency and amplitude frequency at which maximal coupling occurred for each of the LFP recordings demonstrating significant PAC and found no differences between PD and dystonia (PD vs. dystonia, phase frequency: $p = 0.7718$; amplitude frequency: $p = 0.9769$, MI: $p = 0.5632$; Wilcoxon rank sum test; Fig. 3C).

We also investigated the consistency with which the coupling occurred for a specific phase of beta oscillation. For significantly coupled beta-HFO phase-amplitude pairs, the phase at which the phase-amplitude distribution was maximal was calculated and averaged for alpha, low beta, and high beta bands. The resulting mean phase angles were plotted on a radial histogram for each recording ($n = 19$, PD; $n = 6$, dystonia). The phase at which coupling occurred was variable across individual subjects for both disease states (Fig. 3D). Although the radial histograms suggest the possibility of opposite preferred phases, this was not significant (PD vs. dystonia median phase angle: alpha: $p > 0.1$, low beta: $p > 0.1$, high beta: $p = 0.1000$, Kuiper's test).

3.5. No difference between focal and generalized forms of dystonia

It is possible that the putative biomarkers of the parkinsonian state explored here could share considerable overlap with isolated dystonia,

Table 2
Clinical characteristics of dystonia patients.

Pt #	Age	Sex	Side recorded	Dystonia Type	Disease duration (years)	Dyt medication	TWSTRS	BFMDRS	Lead location[a] (mm)		
									Lat	AP	Vert
1	48	F	Right	Cervical	4	None	22	8	11.5	−3.5	−0.7
2	65	F	Left	Craniocervical	6	Lorazepam	15	13.5	−10.4	0.0	−0.5
3	66	M	Right	Craniocervical	3	Lorazepam, baclofen	23	23	11.7	−0.5	−3.2
4	71	M	Left	Cervical	30	Lorazepam	23	13	−15.1	−2.7	−2.1
5	40	F	Left	Cervical	9	Clonazepam	24	8	−11.7	−2.9	−1.5
6	55	F	Right	Craniocervical	3	Diazepam, alprazolam	16	13	11.0	−2.3	−2.2
7	53	F	Left	DYT1 + generalized	32	Alprazolam, tizanidine	0	5	−12.1	−0.1	−1.4
8	53	M	Left	Generalized	28	Alprazolam, clonazepam	21	15	−13.4	−0.6	−0.7
9	46	M	Right	DYT1 + generalized	28	Sinemet[b], propranolol, Primidone, clonazepam	13	7	11.5	0.1	−1.4
10	64	M	Right	Generalized	10	Clonazepam	na	na	13.0	−0.9	−1.2
11	16	M	Left	DYT1 + generalized	7	Artane	9	21.5	−13.4	−0.4	−2.9
12	63	M	Right	Generalized	15	Clonazepam, propranolol	13	18.5	12.4	−2.0	−4.7

Dyt medication: medications for dystonia; TWSTERS: Toronto Western Spasmodic Torticollis Rating Scale; BFMDRS: Burke-Fahn-Marsden Dystonia Rating Scale; Lat: lateral distance from mid-commissural point; AP: anterior–posterior distance from mid-commissural point; Vert: vertical distance from mid-commissural point. DYT1 +: DYT1 gene mutation.
[a] Location of the recording contact in anterior commissure and post commissure plane.
[b] Medications for patient 9 were held 2 days prior to surgery. na: not available.

considering some of the pathophysiologic similarities between these two conditions (Miocinovic et al., 2015). Thus, a failure of these biomarkers to distinguish between the two disease states does not necessarily invalidate their utility as a biomarker. If elements of STN beta activity are reflective of the severity of basal ganglia disease in general, we might expect them to differ between more severe generalized forms of dystonia and focal cervical or segmental craniocervical dystonia. However, we found no systematic differences in the power, width, or peak frequency of the alpha-beta peak in focal/segmental dystonia ($n = 6$) versus generalized forms ($n = 6$) (Focal vs. generalized: amplitude: $p = 0.8182$, frequency: $p = 0.5563$; width: $p = 0.9372$; Wilcoxon rank sum test; Fig. 2E). Significant PAC was found in two of six focal/segmental dystonia and four of six generalized dystonia recordings without differences in MI or frequency of maximum PAC.

4. Discussions

We used resting state LFP recordings from the STN of patients undergoing DBS surgery for movement disorders to evaluate LFP features that have been proposed as biomarkers for the parkinsonian state. Comparing STN LFP recordings in patients with akinetic-rigid PD to those with isolated dystonia, we found that the amplitude, width, and frequency of the beta peak in the LFP power spectrum did not distinguish disease groups. The coupling of beta phase to HFO amplitude, proposed to be a

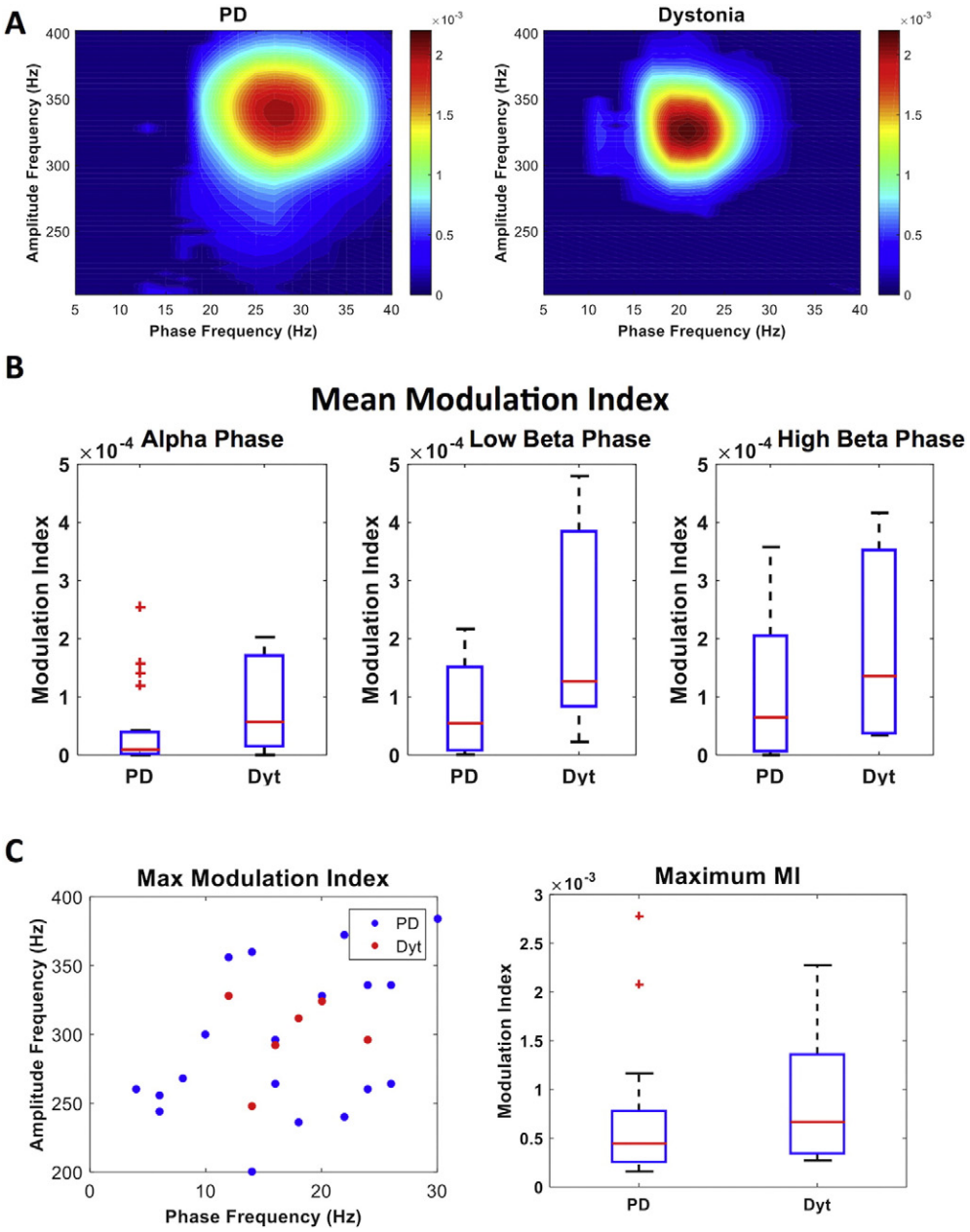

Fig. 3. — STN phase amplitude coupling (PAC) in PD vs dystonia. A) Example comodulograms for PD (left) and dystonia (right) showing high modulation index (MI) between beta phase frequency and high frequency oscillation (HFO) amplitude. Warmer color demonstrates higher MI values. B) Boxplots of beta-HFO PAC in subjects who had detectable PAC (19/28 PD patients, 6/12 dystonia patients). There was no significant difference between groups (PD vs. dystonia: alpha: $p = 0.4011$; low beta, $p = 0.2035$; high beta $p = 0.3547$; Wilcoxon rank sum test). C) (Left) Scatter plot of the phase and amplitude where maximal MI occurs (PD vs. dystonia: phase frequency, $p = 0.7718$; amplitude frequency, $p = 0.9769$; Wilcoxon rank sum test). (Right) Boxplots of maximal modulation index for PD and dystonia (PD vs. dystonia: $p = 0.5632$; Wilcoxon rank sum test). D) Polar histograms showing averaged phase angle for those phase and amplitude frequency pairs showing significant PAC in 19 PD patients (top) and 6 dystonia (bottom). Red line indicates median phase angle and shaded area indicates standard deviation. There is no statistical difference among the groups in phase preference (PD vs. dystonia, $p > 0.1$ for alpha and low beta phase, $p = 0.1000$ high beta phase, Kuiper's test).

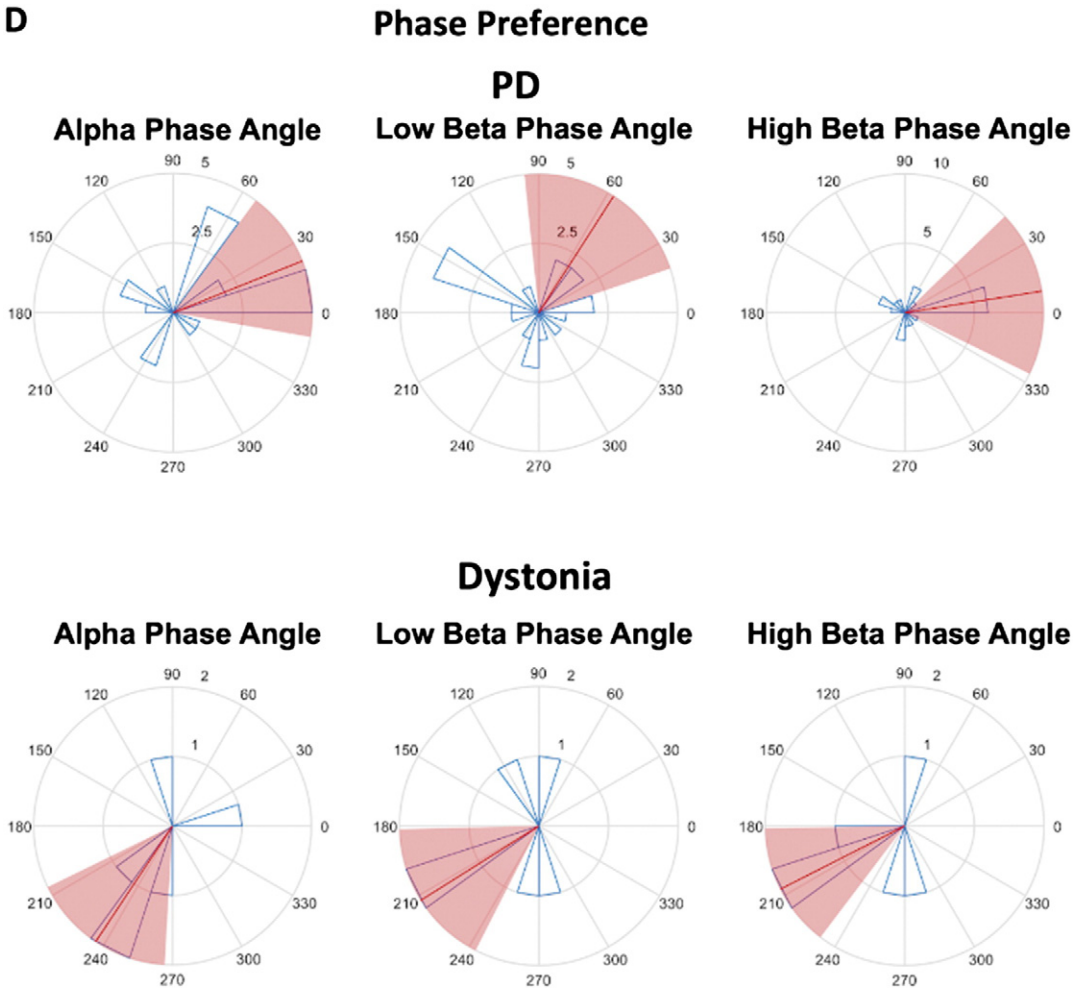

Fig. 3 (*continued*).

biomarker for PD, was also present in isolated dystonia. Our findings suggest that these metrics of beta band activity are not specific to the parkinsonian state.

4.1. Beta oscillations in the STN LFP: a specific biomarker?

The reduction in the amplitude of beta oscillations with dopamine replacement therapy and DBS has been the basis for the theory that higher amplitude beta oscillations emerge following dopamine depletion, and that this is a key component of the circuit abnormalities underlying the motor signs of PD (Giannicola et al., 2010; Kuhn et al., 2008; Priori et al., 2004). This view is appealing in part because beta band activity in the motor and premotor areas is pronounced during the maintenance of posture, and greatly reduced during fluid movements (Chakarov et al., 2009; Klostermann et al., 2007; Sanes and Donoghue, 1993). Thus, exaggerated beta activity could lead to the inability to switch between different states (Engel and Fries, 2010). In several rodent models of PD, dopamine depletion does result in an increase in the amplitude of beta oscillations in several structures in the basal ganglia-thalamocortical loop (Costa et al., 2006; Mallet et al., 2008). However, other studies using progressive model of parkinsonism in rodents and non-human primates showed equivocal changes in beta oscillations (Connolly et al., 2015; Devergnas et al., 2014; Leblois et al., 2007; Leventhal et al., 2012). Although the amplitude of beta oscillations in the LFP power spectrum is reduced by successful therapy in humans, this reduction should not necessarily be interpreted as returning the STN to its "normal" state. Instead, the reduction in STN beta power by oral levodopa and by DBS may represent a nonphysiological compensatory pathway toward interrupting a more fundamental abnormality of the parkinsonian state, that of excessive spike synchronization to beta phase throughout the basal ganglia and motor cortex (de Hemptinne et al., 2013; Kuhn et al., 2005; Moran et al., 2008; Shimamoto et al., 2013; Weinberger et al., 2006). Spike synchronization to beta phase is likely to be a more specific biomarker, although one that is not as practical to study as LFP power. Of note, greater entrainment of spiking activity to beta phase throughout the motor circuit does not necessarily require an increase in the amplitude of beta oscillations in all structures of the circuit; rather, increased beta phase coherence throughout the network could produce such entrainment (Silberstein et al., 2005).

In humans, there has been no direct evidence that the presence of a prominent beta peak in the STN LFP power spectrum is a parkinsonian state-specific biomarker. Our results cast doubt on the disease specificity of the properties of the STN LFP examined in this study, and are consistent with two possibilities: that these properties are abnormal but are common to both PD and dystonia, or that they represent normal STN physiology. Although invasive studies of basal ganglia physiology in healthy humans are ethically impossible, analysis of STN LFPs in additional disease states, such as obsessive–compulsive disorder (Bastin et al., 2014), may help to distinguish between these interpretations.

4.2. LFP biomarkers in other motor structures

Our results do not rule out the possibility that the power of LFP beta oscillations in other structures of the motor system could be elevated in PD compared to other disorders. A few studies have examined LFP

characteristics in isolated dystonia patients undergoing globus pallidus pars interna (GPi) DBS implantation (Chen et al., 2006a; Chen et al., 2006b; Liu et al., 2008; Silberstein et al., 2003) and found higher oscillatory activity in the 4–12 Hz range in dystonia, which correlates with involuntary EMG activity. The lack of increased theta power in the STN of dystonia patients could be due to differences in inputs between the GPi and STN. In two studies that directly compared GPi LFP in PD and dystonia, spectral power in the beta band was relatively higher in PD than in isolated dystonia (Silberstein et al., 2003; Weinberger et al., 2012). However, one of these studies also showed that a discrete peak was found consistently in the 11–30 Hz range in both disease groups, and that synchronization of neuronal firing with LFP oscillations is a more prominent feature in PD than in dystonia (Weinberger et al., 2012). In a recent study of MPTP-induced parkinsonism in nonhuman primates, resting state beta oscillations were present in the naïve pallidum, and after induction of parkinsonism, beta band power was not correlated with disease severity (Connolly et al., 2015). Future studies comparing LFP oscillations and spike-field relationships in different movement disorders may clarify the disease specificity of biomarkers in the pallidum.

4.3. Phase-amplitude coupling in the STN

In normal cortical physiology, PAC is an important mechanism for communication within and between neuron ensembles in different brain regions by coordinating timing of neuronal activity in connected networks (Canolty et al., 2010; Canolty and Knight, 2010). Excessive coupling may entrain neuronal firing in an inflexible pattern that limits information encoding by spatiotemporal selectivity (Litvak et al., 2011). In the parkinsonian motor cortex, excessive coupling between beta band phase and broadband gamma (50–200 Hz) amplitude has been demonstrated (de Hemptinne et al., 2013), and this has been interpreted as a reflection of the elevated synchronization of population spiking at beta frequencies that occurs through the motor system in PD (Levy et al., 2002; Moran et al., 2008; Weinberger et al., 2006).

In the basal ganglia, there is also interest in the possibility that other types of PAC may represent parkinsonian biomarkers. The coupling of beta phase to the amplitude of HFOs has been seen in STN LFPs and can be modulated by dopaminergic state (Lopez-Azcarate et al., 2010). However, the physiological interpretation of STN PAC may be quite different from that of cortical PAC, since the former involved the amplitude of a very high frequency oscillation (250–350 Hz), while the latter involves the amplitude of broadband activity (50–200 Hz), rather than an oscillatory rhythm. A recent study cast doubt on the view that that beta-HFO coupling in the STN represents a marker of spike synchronization (Yang et al., 2014).

Here, we found significant PAC in 19/28 LFP recordings in PD (68%) and 6/12 in dystonia (50%), suggesting that beta-HFO PAC in the STN LFP is not a specific parkinsonian biomarker. The fact that PAC was absent in several patients in each group is consistent with a previous study demonstrating that PAC is greatest at the dorsal STN border in PD patients and that the percentage of recordings with significant PAC ranged between ~40–60% depending on the relative depth of recording electrode within the STN (Yang et al., 2014). Here, we only recorded LFPs at a single site in STN. This does not rule out the possibility that beta-HFO PAC could be an important marker in other basal ganglia nuclei. In MPTP-induced nonhuman primate model of Parkinsonism, emergence of beta-HFO coupling in the pallidum occurred in the mild state and increased with symptom severity (Connolly et al., 2015).

4.4. Limitations

All recordings were performed in a state of alert rest in the intraoperative setting, at least 30 min after stopping propofol. While there are effects of propofol on STN neuronal activity (Raz et al., 2010) and STN LFP activity (Swann et al., 2016), the half- life for propofol elimination is short (Kanto and Gepts, 1989). Further, the majority of patients had LFP recorded on the second side during bilateral DBS implantation surgery (24/28 PD patients and 9/12 dystonia patients), which was >2 h after cessation of propofol. Many of the dystonia patients were on chronic benzodiazepines which may have the effect of increasing beta oscillations in the motor system (Yamadera et al., 1993). Cessation of medication for 12 h may not be sufficient time for those PD patients taking dopamine (DA) agonists to be in the full OFF state. However, comparison of those on DA agonists (19 patients) to those who were not (9 patients) did not reveal differences in putative biomarkers (Supplementary Fig. 5A–C). Data were also collected on macroelectrodes after MER recording, which can lead to microlesional effects that results in symptom improvement (Koop et al., 2006). The majority of patients underwent a single MER pass per side (20/28 PD patients and 9/12 dystonia patients) prior to DBS lead insertion. Others have quantified the changes in LFP spectral power overtime post-implantation showing no changes in low beta or high beta power between time of implantation to 48 h or 30 days after surgery (Rosa et al., 2010). The intraoperative environment may produce a heightened emotional state such that LFP characteristics differ from those recorded postoperatively through temporarily externalized leads. Additionally, differences in physiological recording systems used during the study increased data set variability, but we did not observe any specific trends with respect to the recording system used. Because we limited our study to those patients without significant tremor during recordings to avoid the possible confound introduced by movement related changes in LFP characteristics (Kuhn et al., 2004; Qasim et al., 2015), our results may not be generalizable to all PD or dystonia patients. While we have the largest series of STN recordings from isolated dystonia patients to date, our sample size might still be underpowered to detect small differences in the parameters evaluated. Because both isolated dystonia and PD are movement disorders, STN-LFP recordings from patients without movement disorders would be very valuable for comparison, but are rare (Bastin et al., 2014).

5. Conclusions

LFPs recorded from the STN of PD and isolated dystonia patients demonstrate that both diseases show prominent beta band spectral peaks and coupling between beta-phase and HFO amplitude. These features of beta oscillations recorded in the STN LFP may be important in the pathophysiology of basal ganglia disorders, but are not specific diagnostic biomarkers for the parkinsonian state. Other beta band phenomena, such as spike-field interactions may be more specific to PD. Our results do not contradict prior findings that STN LFP characteristics change with successfully therapy in PD, and do not rule out the possibility that beta oscillatory phenomena may prove useful as control signals in feedback controlled deep brain stimulation (Little et al., 2013).

Supplementary data to this article can be found online at http://dx.doi.org/10.1016/j.nbd.2016.02.015.

References

Bastin, J., et al., 2014. Changes of oscillatory activity in the subthalamic nucleus during obsessive–compulsive disorder symptoms: two case reports. Cortex 60, 145–150.

Bergman, H., et al., 1994. The primate subthalamic nucleus. II. Neuronal activity in the MPTP model of parkinsonism. J Neurophysiol. 72, 507–520.

Bronte-Stewart, H., et al., 2009. The STN beta-band profile in Parkinson's disease is stationary and shows prolonged attenuation after deep brain stimulation. Exp. Neurol. 215, 20–28.

Cagnan, H., et al., 2015. The relative phases of basal ganglia activities dynamically shape effective connectivity in Parkinson's disease. Brain 138, 1667–1678.

Canolty, R.T., Knight, R.T., 2010. The functional role of cross-frequency coupling. Trends Cogn. Sci. 14, 506–515.

Canolty, R.T., et al., 2010. Oscillatory phase coupling coordinates anatomically dispersed functional cell assemblies. Proc. Natl. Acad. Sci. U. S. A. 107, 17356–17361.

Chakarov, V., et al., 2009. Beta-range EEG–EMG coherence with isometric compensation for increasing modulated low-level forces. J. Neurophysiol. 102, 1115–1120.

Chen, C.C., et al., 2006a. Oscillatory pallidal local field potential activity correlates with involuntary EMG in dystonia. Neurology 66, 418–420.

Chen, C.C., et al., 2006b. Neuronal activity in globus pallidus interna can be synchronized to local field potential activity over 3–12 Hz in patients with dystonia. Exp. Neurol. 202, 480–486.

Chen, C.C., et al., 2007. Excessive synchronization of basal ganglia neurons at 20 Hz slows movement in Parkinson's disease. Exp. Neurol. 205, 214–221.
Connolly, A.T., et al., 2015. Modulations in oscillatory frequency and coupling in globus pallidus with increasing parkinsonian severity. J Neurosci. 35, 6231–6240.
Costa, R.M., et al., 2006. Rapid alterations in corticostriatal ensemble coordination during acute dopamine-dependent motor dysfunction. Neuron 52, 359–369.
Danish, S.F., et al., 2007. High-frequency oscillations (>200 Hz) in the human non-parkinsonian subthalamic nucleus. Brain Res. Bull. 74, 84–90.
de Hemptinne, C., et al., 2013. Exaggerated phase-amplitude coupling in the primary motor cortex in Parkinson disease. Proc. Natl. Acad. Sci. U. S. A. 110, 4780–4785.
de Hemptinne, C., et al., 2015. Therapeutic deep brain stimulation reduces cortical phase-amplitude coupling in Parkinson's disease. Nat. Neurosci. 18, 779–786.
Devergnas, A., et al., 2014. Relationship between oscillatory activity in the cortico-basal ganglia network and parkinsonism in MPTP-treated monkeys. Neurobiol. Dis. 68, 156–166.
Engel, A.K., Fries, P., 2010. Beta-band oscillations—signalling the status quo? Curr. Opin. Neurobiol. 20, 156–165.
Galvan, A., et al., 2015. Alterations in neuronal activity in basal ganglia-thalamocortical circuits in the parkinsonian state. Front. Neuroanat. 9, 5.
Giannicola, G., et al., 2010. The effects of levodopa and ongoing deep brain stimulation on subthalamic beta oscillations in Parkinson's disease. Exp. Neurol. 226, 120–127.
Hammond, C., et al., 2007. Pathological synchronization in Parkinson's disease: networks, models and treatments. Trends Neurosci. 30, 357–364.
Hanson, T.L., et al., 2012. Subcortical neuronal ensembles: an analysis of motor task association, tremor, oscillations, and synchrony in human patients. J Neurosci. 32, 8620–8632.
Kanto, J., Gepts, E., 1989. Pharmacokinetic implications for the clinical use of propofol. Clin. Pharmacokinet. 17, 308–326.
Klostermann, F., et al., 2007. Task-related differential dynamics of EEG alpha- and beta-band synchronization in cortico-basal motor structures. Eur J Neurosci. 25, 1604–1615.
Koop, M.M., et al., 2006. Improvement in a quantitative measure of bradykinesia after microelectrode recording in patients with Parkinson's disease during deep brain stimulation surgery. Mov. Disord. 21, 673–678.
Kuhn, A.A., et al., 2004. Event-related beta desynchronization in human subthalamic nucleus correlates with motor performance. Brain 127, 735–746.
Kuhn, A.A., et al., 2005. The relationship between local field potential and neuronal discharge in the subthalamic nucleus of patients with Parkinson's disease. Exp. Neurol. 194, 212–220.
Kuhn, A.A., et al., 2008. High-frequency stimulation of the subthalamic nucleus suppresses oscillatory beta activity in patients with Parkinson's disease in parallel with improvement in motor performance. J Neurosci. 28, 6165–6173.
Leblois, A., et al., 2007. Late emergence of synchronized oscillatory activity in the pallidum during progressive Parkinsonism. Eur J Neurosci. 26, 1701–1713.
Leventhal, D.K., et al., 2012. Basal ganglia beta oscillations accompany cue utilization. Neuron 73, 523–536.
Levy, R., et al., 2002. Synchronized neuronal discharge in the basal ganglia of parkinsonian patients is limited to oscillatory activity. J Neurosci. 22, 2855–2861.
Little, S., et al., 2012. Beta band stability over time correlates with Parkinsonian rigidity and bradykinesia. Exp. Neurol. 236, 383–388.
Little, S., et al., 2013. Adaptive deep brain stimulation in advanced Parkinson disease. Ann. Neurol. 74, 449–457.
Litvak, V., et al., 2011. Resting oscillatory cortico-subthalamic connectivity in patients with Parkinson's disease. Brain 134, 359–374.
Liu, X., et al., 2008. The sensory and motor representation of synchronized oscillations in the globus pallidus in patients with primary dystonia. Brain 131, 1562–1573.
Lopez-Azcarate, J., et al., 2010. Coupling between beta and high-frequency activity in the human subthalamic nucleus may be a pathophysiological mechanism in Parkinson's disease. J Neurosci. 30, 6667–6677.
Mallet, N., et al., 2008. Disrupted dopamine transmission and the emergence of exaggerated beta oscillations in subthalamic nucleus and cerebral cortex. J Neurosci. 28, 4795–4806.
Miocinovic, S., et al., 2015. Patterns of cortical synchronization in isolated dystonia compared with Parkinson disease. JAMA Neurol.
Moran, A., et al., 2008. Subthalamic nucleus functional organization revealed by parkinsonian neuronal oscillations and synchrony. Brain 131, 3395–3409.
Nini, A., et al., 1995. Neurons in the globus pallidus do not show correlated activity in the normal monkey, but phase-locked oscillations appear in the MPTP model of parkinsonism. J. Neurophysiol. 74, 1800–1805.
Ostrem, J.L., et al., 2011. Subthalamic nucleus deep brain stimulation in primary cervical dystonia. Neurology 76, 870–878.
Ozkurt, T.E., et al., 2011. High frequency oscillations in the subthalamic nucleus: a neurophysiological marker of the motor state in Parkinson's disease. Exp. Neurol. 229, 324–331.
Priori, A., et al., 2004. Rhythm-specific pharmacological modulation of subthalamic activity in Parkinson's disease. Exp. Neurol. 189, 369–379.
Qasim, S.E., et al., 2015. Electrocorticography reveals beta desynchronization in the basal ganglia-cortical loop during rest tremor in Parkinson's disease. Neurobiol. Dis. 86, 177–186.
Raz, A., et al., 2010. Propofol decreases neuronal population spiking activity in the subthalamic nucleus of Parkinsonian patients. Anesth. Analg. 111, 1285–1289.
Rosa, M., et al., 2010. Time dependent subthalamic local field potential changes after DBS surgery in Parkinson's disease. Exp. Neurol. 222, 184–190.
Rowland, N.C., et al., 2015. Task-related activity in sensorimotor cortex in Parkinson's disease and essential tremor: changes in beta and gamma bands. Front. Hum. Neurosci. 9, 512.
Sanes, J.N., Donoghue, J.P., 1993. Oscillations in local field potentials of the primate motor cortex during voluntary movement. Proc. Natl. Acad. Sci. U. S. A. 90, 4470–4474.
Shimamoto, S.A., et al., 2013. Subthalamic nucleus neurons are synchronized to primary motor cortex local field potentials in Parkinson's disease. J Neurosci. 33, 7220–7233.
Silberstein, P., et al., 2003. Patterning of globus pallidus local field potentials differs between Parkinson's disease and dystonia. Brain 126, 2597–2608.
Silberstein, P., et al., 2005. Cortico-cortical coupling in Parkinson's disease and its modulation by therapy. Brain 128, 1277–1291.
Stanslaski, S., et al., 2012. Design and validation of a fully implantable, chronic, closed-loop neuromodulation device with concurrent sensing and stimulation. IEEE Trans. Neural Syst. Rehabil. Eng. 20, 410–421.
Starr, P.A., 2002. Placement of deep brain stimulators into the subthalamic nucleus or Globus pallidus internus: technical approach. Stereotact. Funct. Neurosurg. 79, 118–145.
Swann, N.C., et al., 2016. Motor system interactions in the beta band decrease during loss of consciousness. J. Cogn. Neurosci. 28, 84–95.
Tort, A.B., et al., 2010. Measuring phase-amplitude coupling between neuronal oscillations of different frequencies. J. Neurophysiol. 104, 1195–1210.
Weinberger, M., et al., 2006. Beta oscillatory activity in the subthalamic nucleus and its relation to dopaminergic response in Parkinson's disease. J. Neurophysiol. 96, 3248–3256.
Weinberger, M., et al., 2012. Oscillatory activity in the globus pallidus internus: comparison between Parkinson's disease and dystonia. Clin. Neurophysiol. 123, 358–368.
Wingeier, B., et al., 2006. Intra-operative STN DBS attenuates the prominent beta rhythm in the STN in Parkinson's disease. Exp. Neurol. 197, 244–251.
Yamadera, H., et al., 1993. Pharmaco-EEG mapping of diazepam effects using different references and absolute and relative power. Pharmacopsychiatry 26, 254–258.
Yang, A.I., et al., 2014. Beta-coupled high-frequency activity and beta-locked neuronal spiking in the subthalamic nucleus of Parkinson's disease. J Neurosci. 34, 12816–12827.